Metallomics

Accepted Manuscript

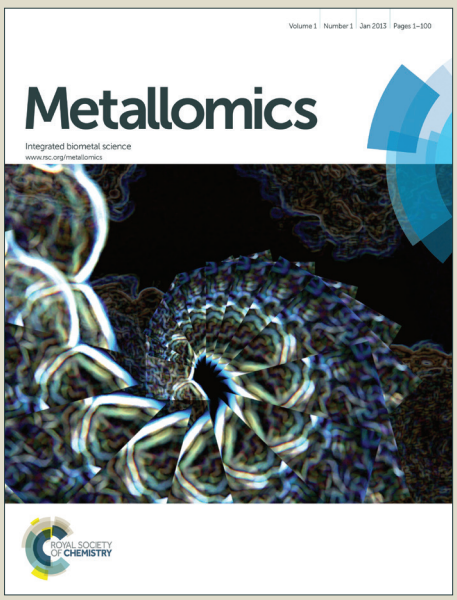

ROYAL SOCIETY OF CHEMISTRY

www.rsc.org/metallomics

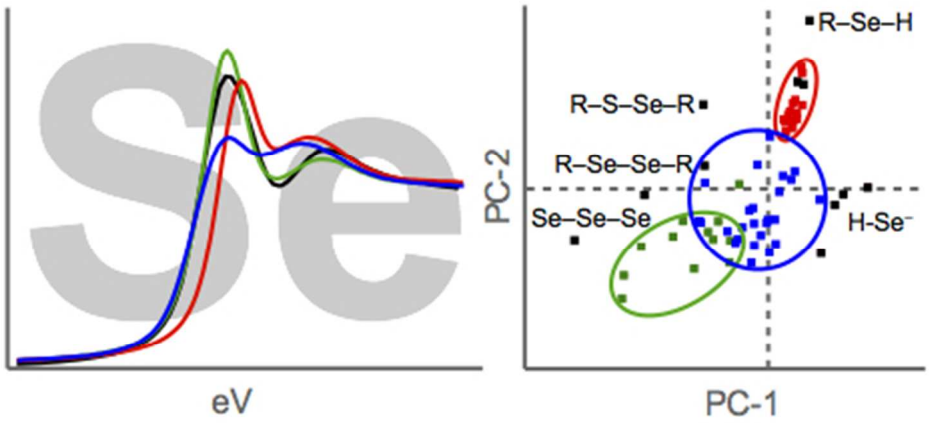

An investigation of selenium speciation in the tissues of selenite-fed rats by principal component analysis of X-ray absorption spectra.
79x39mm (150 x 150 DPI)

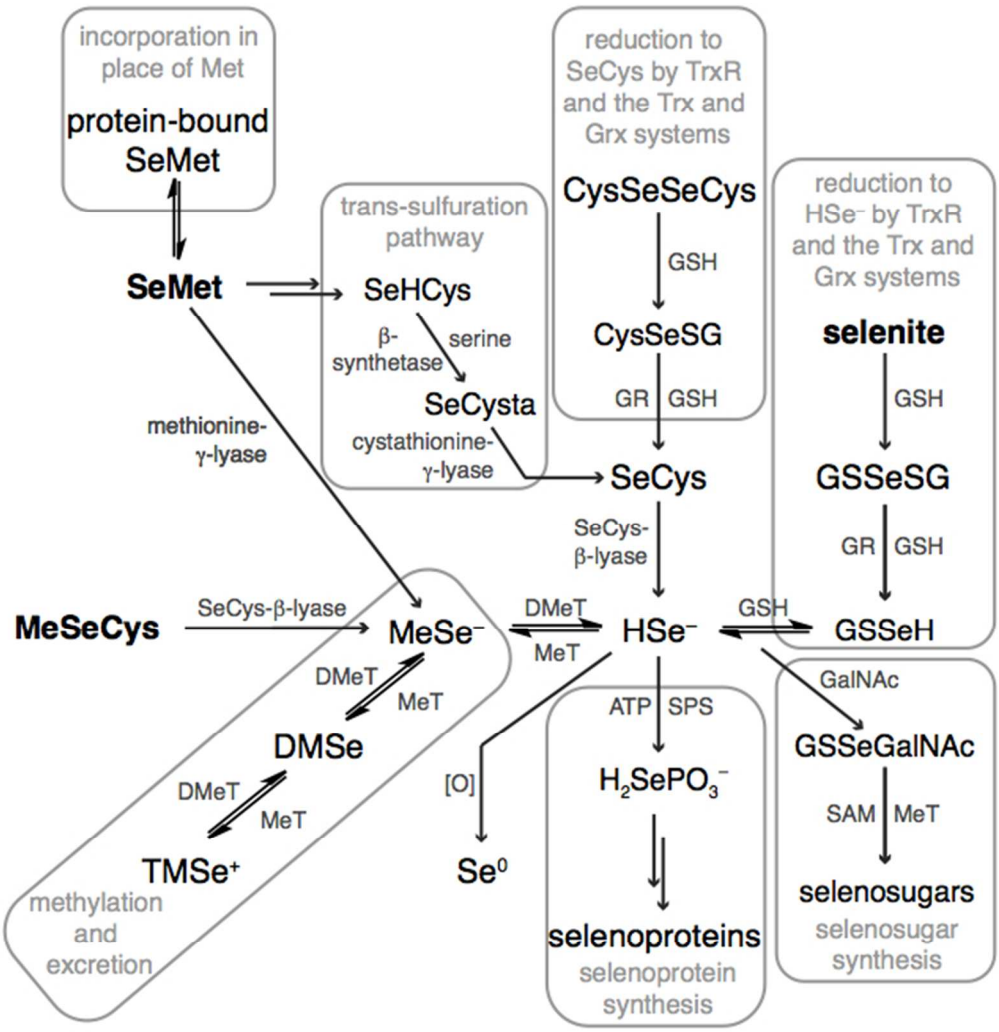

The metabolic pathways of the dietary selenium compounds. Abbreviations: CysSeSG, selenocysteine-glutathione selenenylsulfide; DeMeT, DMSe, dimethylselenide; demethyltransferases; GalNAc, *N*-acetylgalactosamine; GR, glutathione reductase; GSSeGalNAc, Glutathionylseleno-*N*-acetylgalactosamine; $H_2SePO_3^-$, monoselenophosphate; $MeSe^-$, methylselenolate; MeT, methyltransferases; SAM, S-Adenosyl-L-methionine; SeCysta, selenocystathionine; SeHCys, selenohomocysteine; SPS, selenophosphate synthetase. Adapted from Ref. 48. Refer to the aforementioned reference for more detail on the scheme and references to the in vitro and in vivo experiments from which the scheme is derived.
107x112mm (150 x 150 DPI)

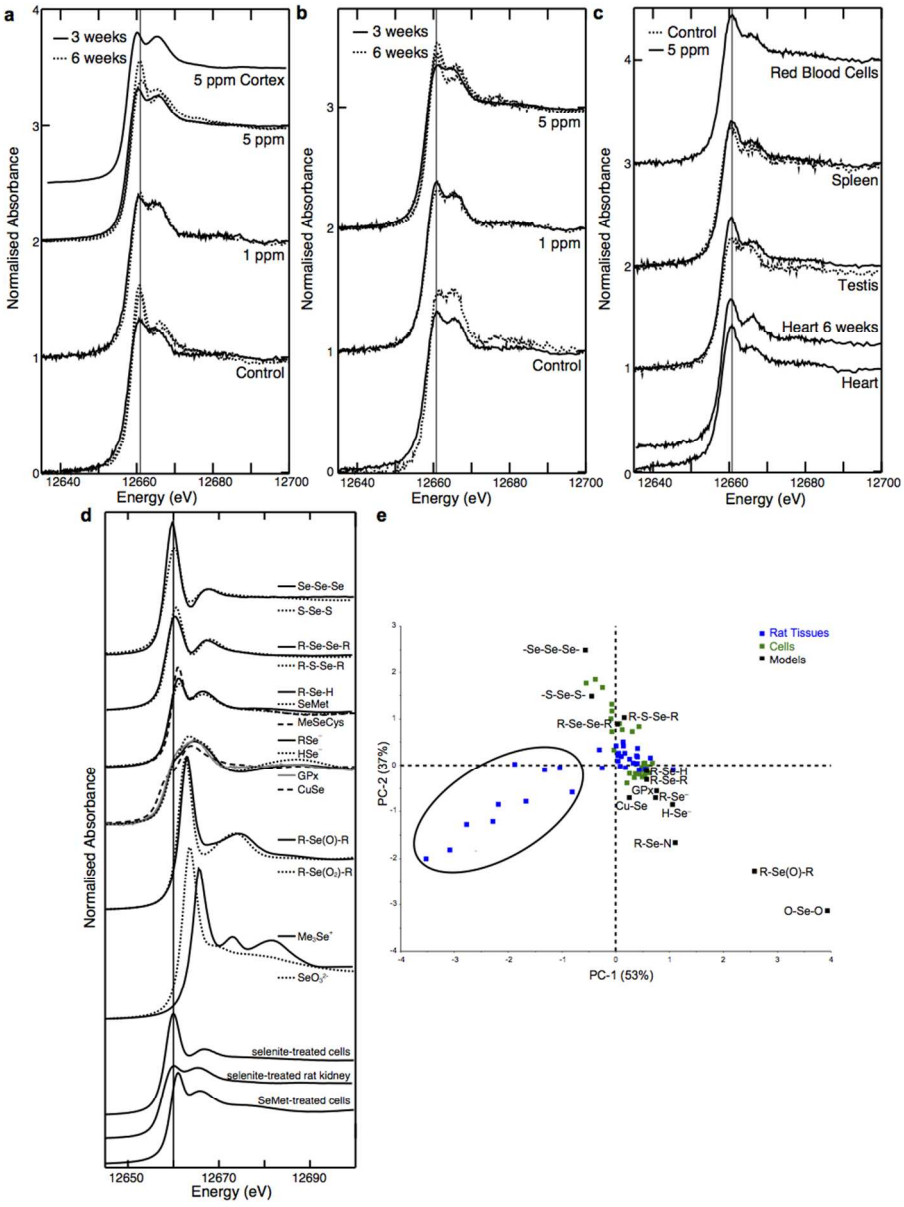

Se K-edge XANES spectra of (a) kidney, (b) liver and (c) red blood cells, spleen, testis or heart tissues from rats fed control, 1 ppm or 5 ppm Se (as selenite) diets for 3 or 6 weeks. Se K-edge XANES spectra of (d) model Se compounds, selected selenite-treated and SeMet-treated cell spectra and the spectrum from a kidney of a rat fed a 5 ppm selenite diet. The model compounds for each coordination environment are as follows: elemental Se (Se–Se–Se), GSSeSG (S–Se–S), CysSeSeCys (R–Se–Se–R), CysSSeCys (R–S–Se–R), SeCys (R–Se–H), SeMet and MeSeCys (R–Se–R), $CysSe^-$ (RSe^-), Me_2SeO (R–Se(O)–R) and Me_2SeO_2 (R–$Se(O_2)$–R), $TMSe^+$ (R_3–Se^+) and SeO_3^{2-}. PCA scores plot (e) of XANES spectra of cells treated with Se compounds (selenite, SeMet and MeSeCys); tissues of rats fed control, 1 ppm or 5 ppm Se (as selenite) diets; and Se model compounds. Circled in black are the spectra lying outside the axis defined by the spread of the model Se compounds. See Figure S1 for the XAS spectra of the circled samples. The peak positions of the selenium model compound and selected samples are listed in Table S1. Note that the R–$Se(O_2)$–R and R_3Se^+ models were excluded from PCA as they plotted extremely distantly from the positions of the experimental spectra in the scores plots.

168x224mm (150 x 150 DPI)

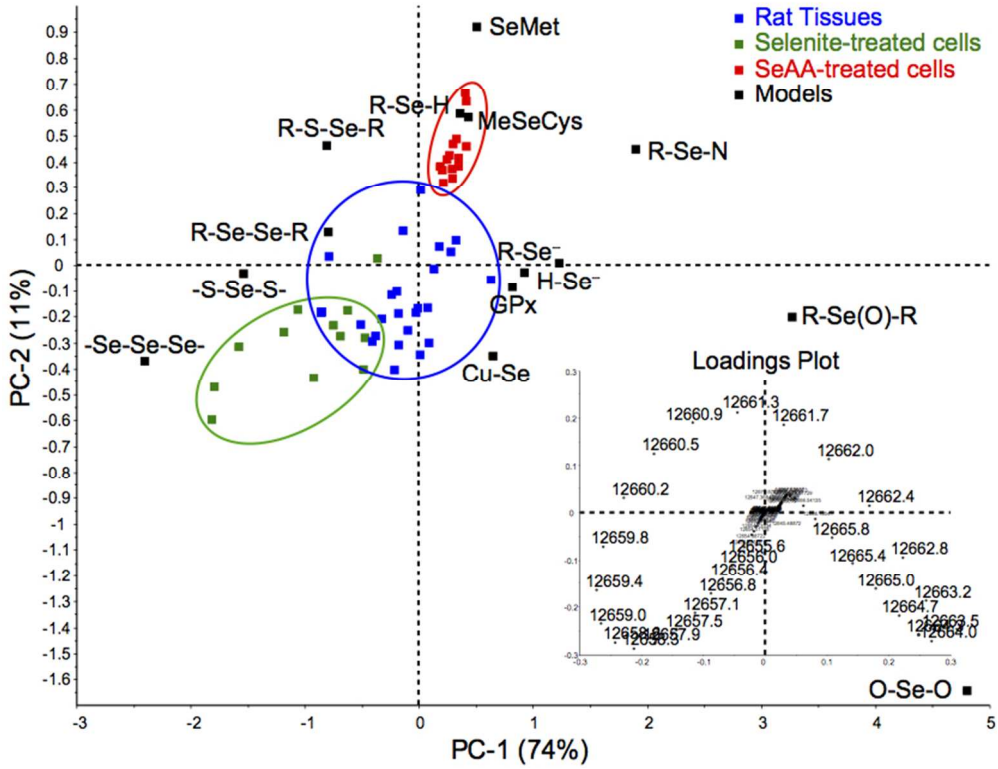

. PCA scores and (inset) loadings plot of XANES spectra of cells treated with selenite or selenoamino acids (SeAA) SeMet and MeSeCys; tissues of rats fed control, 1 ppm or 5 ppm Se (as selenite) diets; and Se model compounds. Sample groupings are circled for clarity.
141x109mm (150 x 150 DPI)

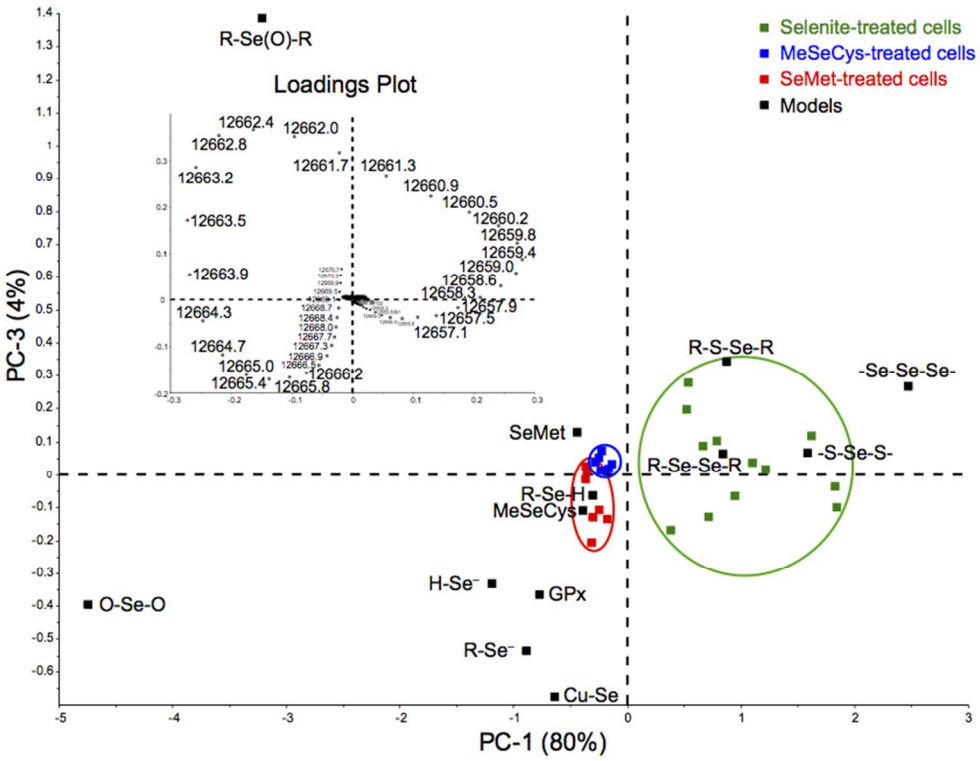

PCA scores and (inset) loadings plot of XANES spectra of cells treated with Se compounds (selenite, SeMet and MeSeCys) and Se model compounds. Sample groupings are circled for clarity – rat tissue spectra are not included in this plot.
145x112mm (150 x 150 DPI)

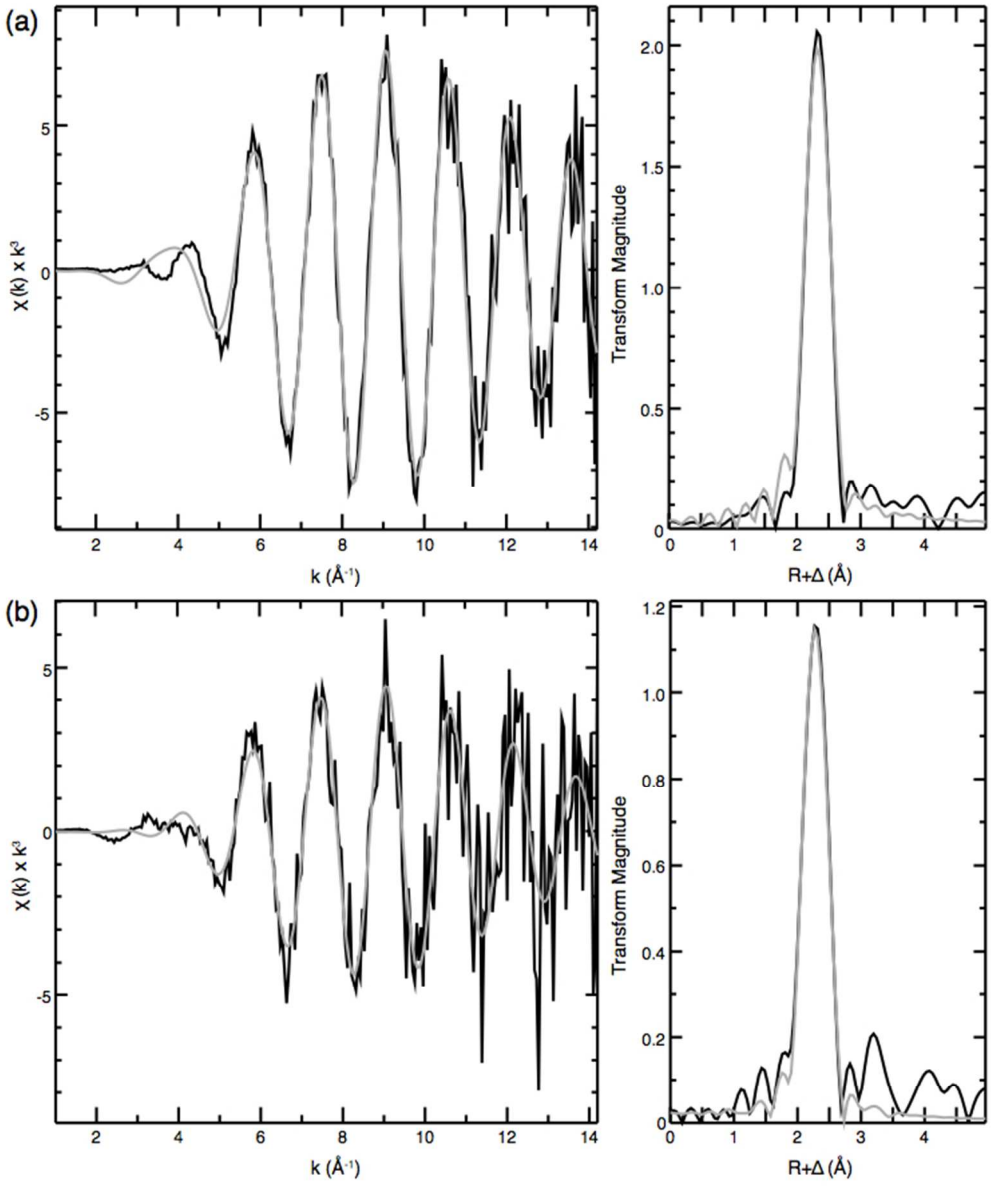

Se K-edge EXAFS spectra of (a) kidney and (b) liver from rats fed a 5 ppm Se (as selenite) diet for 3 weeks. The experimental EXAFS spectra (left, black line) and Fourier Transforms (right, black line) are shown with their calculated fits (grey line). Fit parameters are listed in Table 1.
126x151mm (150 x 150 DPI)

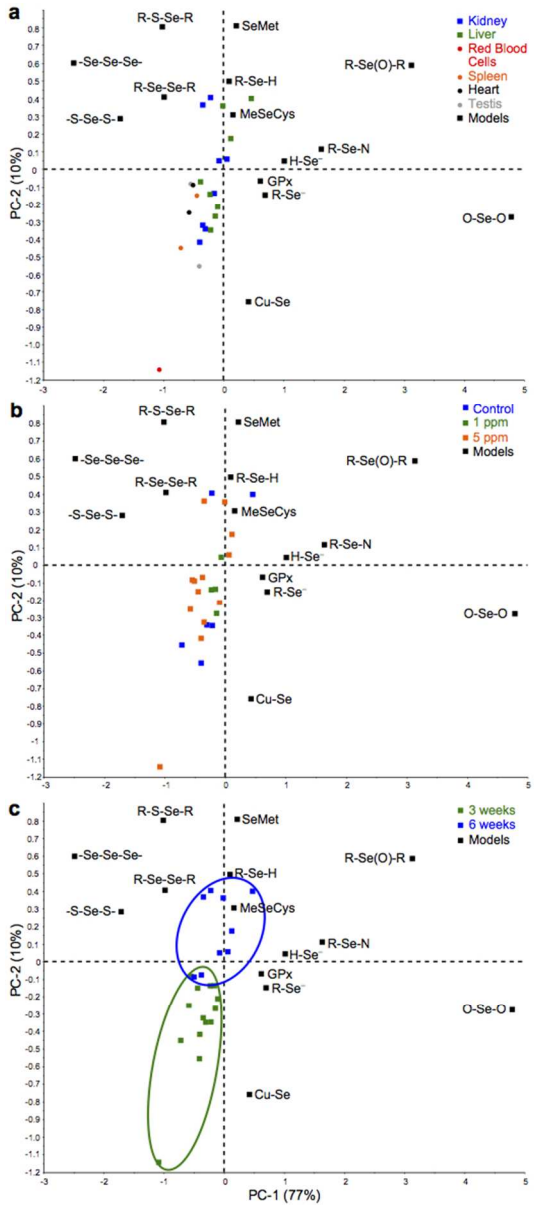

. PCA scores plot of XANES spectra of tissues of rats fed control, 1 ppm or 5 ppm Se (as selenite) diets and Se model compounds. The (a) tissue type, (b) Se dose or (c) duration of the Se diet is indicated. The duration of the Se diet (3 weeks or 6 weeks) is indicated and sample groupings are circled for clarity. See Supporting Information for the corresponding loadings plot (Figure S2).
88x200mm (150 x 150 DPI)

XAS Studies of Se Speciation in Selenite-Fed Rats

Claire M. Weekley,[†] Jade B. Aitken,[§] Paul K. Witting,[‡] and Hugh H. Harris[†,*]

[†]*School of Chemistry and Physics, The University of Adelaide, SA 5005, Australia*

[§]*School of Chemistry, The University of Sydney, NSW 2006, Australia*

[‡]*The Discipline of Pathology, Charles Perkins Centre, The University of Sydney, NSW 2006, Australia*

*To whom correspondence should be addressed. Associate Professor Hugh Harris, *School of Chemistry and Physics, The University of Adelaide, SA 5005, Australia* Phone: 61-08-83135060; Facsimile: 61-8-83134358; Email: hugh.harris@adelaide.edu.au

Abstract

The biological activity of selenium is dependent on its chemical form. Therefore, knowledge of Se chemistry *in vivo* is required for efficacious use of selenium compounds in disease prevention and treatment. Using X-ray absorption spectroscopy, Se speciation in the kidney, liver, heart, spleen, testis and red blood cells of rats fed control (~0.3 ppm Se) or selenite-supplemented (1 ppm or 5 ppm Se) diets for 3 or 6 weeks, was investigated. X-ray absorption spectroscopy revealed the presence of Se–Se and Se–C species in the kidney and liver, and Se–S species in the kidney, but not the liver. X-ray absorption near edge structure (XANES) spectra showed that there was variation in speciation in the liver and kidneys, but Se speciation was much more uniform in the remaining organs. Using principal component analysis (PCA) to interpret the Se K-edge X-ray absorption spectra, we were able to directly compare the speciation of Se in two different models of selenite metabolism – human lung cancer cells and rat tissues. The effects of Se dose, tissue type and duration of diet on selenium speciation in rat tissues were investigated, and a relationship between the duration of the diet (3 weeks *versus* 6 weeks) and selenium speciation was observed.

Abbreviations

EXAFS, extended X-ray absorption fine structure; GPx, glutathione peroxidase; GSSeH, glutathione selenenylsulfide; GSSeSG, selenodiglutathione; MeSeA, methylseleninic acid; MeSeCys, methylselenocysteine; OCT, Optimal Cutting Temperature (compound); PCA, principal component analysis; SeCys, selenocysteine; SelP, selenoprotein P; SeMet, selenomethionine; $TMSe^{+}$, trimethylselenonium; TrxR, thioredoxin reductase; XANES, X-ray absorption near edge structure; XAS, X-ray absorption spectroscopy.

Introduction

Selenium is incorporated into proteins as the 21st amino acid, selenocysteine. As such, Se is essential for the production of selenoproteins, which function as antioxidants (glutathione peroxidases, GPx) and redox modulators (thioredoxin reductases, TrxR) and are involved in Se transport (selenoprotein P, SelP) and thyroid hormone metabolism (iodothyronine deiodinases), amongst other functions.[1] Selenium compounds are under scrutiny due to the involvement of selenoproteins and low molecular weight Se compounds[2] in the prevention and amelioration of diseases including cancer and cardiovascular disease.[3,4] The anticancer and chemopreventative properties of Se in laboratory experiments are clear,[5,6] but the results of clinical trials have been mixed.[7-9]

The biological activity of Se is related to the speciation of the ingested Se compound and its metabolites.[10] Understanding the metabolism and speciation of different Se compounds *in vivo* is necessary for better understanding their varying biological activities.[11] The gap between the efficacies of Se supplementation observed in laboratory studies and in clinical trials may be due, at least in part, to the choice of Se species used in clinical trials. Selenomethionine (SeMet) or selenised yeast (often containing SeMet and other organic Se compounds) are common choices,[12] yet selenite and methylated Se species such as methylselenocysteine (MeSeCys) and methylseleninic acid (MeSeA) are effective chemopreventative compounds in animal studies[5,6,13] – more effective than SeMet.[14] Each of these species has a unique metabolic pathway (see Figure 1 for a comprehensive summary of the metabolic routes of dietary selenium compounds).

The most commonly used methods for investigating Se speciation *in vivo* are chromatographic techniques (primarily liquid chromatography) coupled to mass spectrometry (usually inductively coupled plasma mass spectrometry).[15] These techniques, with the addition of molecular mass spectrometry, are capable of unambiguously identifying Se species, even at trace concentrations[16] and have been used to establish Se speciation in cancer cells and rat hepatocytes treated with selenite, SeMet or MeSeCys.[17,18] Other studies employed stable isotope-labeled Se compounds (including selenite, SeMet and MeSeCys) to study selenium speciation up to 72 h after ingestion.[19-21] In the case of the rat tissues, only the parental compound and some downstream metabolites of a hypothesised common Se intermediate, purportedly HSe^-, have been identified. The downstream metabolites identified included the selenoproteins GPx and SelP, and excretory compounds including trimethylselenonium ($TMSe^+$) and selenosugars. A similar study of Se speciation in rat tissues after a two week MeSeCys diet has been conducted with a similar suite of metabolites identified.[22]

We have used X-ray absorption spectroscopy (XAS) to determine the speciation of Se in human lung cancer and neuroblastoma cells treated with selenite, SeMet or MeSeCys.[23-25] X-ray absorption spectroscopy is capable of determining *in situ* speciation in samples with minimum sample preparation, reducing the risk of the generation of speciation artefacts that may be produced during the sample preparation required for the chromatographic-mass spectrometric techniques. Although X-ray absorption is less sensitive than the chromatographic-mass spectrometric techniques and is limited to determining the coordination environment about the Se atom, it is a technique that can be applied to Se compounds in all states of matter and with minimal sample preparation, thereby avoiding the generation of artefacts.[26]

Having successfully applied XAS to the problem of Se speciation in cancer cells, we are extending the technique to the tissues of rats fed diets containing selenite at different concentrations, with the advantage of being able to directly compare speciation in the two different sample types using the same technique. Selenite differs from organic supplements in that it undergoes reductive metabolism to generate the hypothesised selenide intermediate.[27] Glutathione, TrxR and the TrxR system as well as the glutaredoxin system have all been demonstrated to be involved in the reduction of selenite to hydrogen selenide via selenodiglutathione (GSSeSG) and GSSeH.[28-31] Selenite has been shown to reduce chemical hepatocarcinogenesis[6] and prevent carcinogenesis during the cancer promotion and proliferation phases in rat models.[13] In determining how selenite reduces carcinogenesis, it is important to understand the Se species present in healthy and diseased rats fed high Se diets and how speciation varies with Se dose, tissue type and the duration of the diet.

Herein we report on the speciation of Se in rat tissues using XAS and outline some of the challenges faced. In determining the speciation of Se in cancer cells, we used principal component analysis (PCA) to determine the number of Se species present in the cells, then identified likely models for these species using target transformation before fitting X-ray absorption near edge structure (XANES) spectra with linear combinations of the selected Se model compounds. The *a priori* fitting of extended X-ray absorption fine structure (EXAFS) spectra supported the coordination environment of Se in the cells as determined by XANES fitting. Attempts at fitting XANES spectra of the rat tissues were unsuccessful and due to the low concentrations of Se in most rat tissues, EXAFS was of limited use. Instead, we have applied PCA alone: the linear transformation of the spectral data onto a new coordinate system based on the degree of variance in the data that facilitates visualisation of the data to investigate variation in Se speciation with dose, tissue and treatment duration.

Experimental

Se supplementation

Male Sprague-Dawley rats (80 – 100 g) were from the Animal Resources Centre (Perth, Australia). Animals were acclimated, randomly assigned to groups, and provided a normal diet or sodium selenite supplemented diets ad libitum: 1 ppm or 5ppm prepared by Glen Forrest Specialty Feed (Perth, Western Australia). Normal chow contained ~ 0.3 ppm Se of unknown chemical form, thus the Se-supplemented diets contained a total of 1.3 ppm or 5.3 ppm Se, of which 1 ppm and 5 ppm Se, respectively, was present as selenite. For simplicity the diets will be designated control (no added Se), 1 ppm Se (1 ppm Se added as selenite) and 5 ppm Se (5 ppm Se added as selenite) diets. After 3 weeks of diet, animal weights were: normal chow 230 ± 8 g (n = 4); 1 ppm Se diet 227 ± 8 g (n = 4), and 5 ppm Se diet 217 ± 8 g (n = 4). After 6 weeks of diet, animal weights were: normal chow 337 ± 13 g (n = 4); 1 ppm Se diet 323 ± 5 g (n = 4), and 5 ppm Se diet 313 ± 9 g (n = 4). Studies were conducted with approval from the SWHAS Local Animal Ethics Committee and adhered to NIH Guidelines for the Care and Use of Laboratory Animals.

Harvest of kidneys

Animals were anaesthetised with isofluorane, followed by intraperitoneal injection of ketamine (50mg/kg weight) and xylazine (10 mg/kg weight). A thoracotomy was performed and organs were perfused (phosphate buffer, pH 7.4, 80 mmHg) via the left ventricle with blood flow from the perforated the right atrium. After 2 min, the organs harvested, immersed in Tissue-Tek Optimal Cutting Temperature compound (OCT, ProSciTech, Qld, Australia) and stored at -80°C. Tissues destined for XAS experiments underwent no further preparation.

X-ray absorption spectroscopy

Selenium K-edge X-ray absorption spectra of the tissues were recorded at the Stanford Synchrotron Radiation Lightsource (SSRL), Stanford CA, on beamline 9-3. The X-ray beam was monochromated by diffraction from a pair of Si(220) crystals. Harmonic rejection was achieved by setting the cutoff energy of a Rh-coated mirror to 15 keV. Spectra from frozen whole tissue samples (in OCT) were recorded in fluorescence mode on a 30-element or 100-element Ge detector array (Canberra) at 90° to the incident beam from samples cooled to ~ 10 K in a flowing He cryostat. An As filter (3 absorption path length) and Soller slits were optimally positioned between the sample and the detector to reduce the elastic scatter peak.

The energy ranges used for Se K-edge XANES data collection were: pre-edge region 12425 - 12635 eV (10 eV steps); XANES region 12635 - 12685 eV (0.25 eV steps); and postedge region 12685 - 12872 eV (0.05 $Å^{-1}$ steps in *k*-space). Se K-edge EXAFS spectra were collected at the following energy ranges: pre-edge region 12435 - 12635 eV (10 eV steps); XANES region 12635 - 12685 eV (0.25 eV steps); and EXAFS region 12685 - 13443 eV (0.05 $Å^{-1}$ steps in *k*-space to 14 $Å^{-1}$). A Se foil standard (hexagonal allotrope of Se) was used to calibrate the energy scale to the first peak of the first derivative of the Se edge (12658 eV). Multiple spectra were collected from each sample in order to produce average spectra and increase the signal-to-noise ratio. Sequential spectra from the same samples were compared to ensure that there was no photoreduction of the potentially redox-active Se centres during repeat scans.

The preparation of, and spectroscopic investigations into, Se-treated cancer cells are reported elsewhere.[23-25]

Data analysis

Calibration, averaging and background subtraction of XANES and EXAFS spectra was performed using the EXAFSPAK software package (http://ssrl.slac/stanford.edu/exafspak.html). The energy points in each spectrum were standardised by interpolation using OriginPro 7.5. Principal component analysis was performed on a narrow near-edge region of the spectrum (68 data points between 12645 eV and 12670 eV) using The Unscrambler 10.0.1 (Camo Software, Norway).

Results and Discussion

The concentrations of Se in the kidneys and liver of rats is known to be higher than in other organs.[32,33] The same trend was observed in these experiments, hence the ability to collect EXAFS spectra was limited to tissue from only from the kidney and liver of rats fed the highest Se diet for 3 weeks. We could not collect EXAFS from the same organs of rats fed the 5 ppm Se diet for 6 weeks – the reduction in raw absorbance observed while collecting the data indicated that Se levels were lower in organs from rats on the 6 week high Se diet compared to the 3 week high Se diet.

XANES spectra collected from kidney, liver and other tissues of rats fed control, 1 ppm and 5 ppm Se (as selenite) diets are plotted in Figures 2a, b and c. From these plots, we note that (a) the spectra from the kidney and liver stand apart from the spectra from the remaining tissues both in terms of the relatively high Se concentrations (as judged by the lower noise levels in those spectra)

and in the shape of the spectra and (b) there is substantial variation in the spectra between different samples. The aim of the experiment was to determine whether selenium speciation consistently varied with the duration and concentration of a high Se diet and across different tissues. Typically, speciation is determined from XAS spectra by linear combination fitting of model compound spectra to experimental XANES spectra and *a priori* fitting of EXAFS spectra to determine the average coordination environment of the central atom.

In this case, the fitting of Se K-edge XANES spectra with a linear combination of spectra from a library of Se model compounds proved problematic. The fits for most spectra, regardless of noise level, were poor and thus no useful information was obtained regarding the speciation of Se in the tissues. The poor fits were surprising given the successful fitting of Se-treated cells we have previously reported,[23,24] but comparison of some rat tissue spectra to the spectra of selected Se model compounds and Se-treated cell spectra revealed the distinctly different appearance of the rat tissue spectra (Figure 2d). As opposed to the cell and model compound spectra, which generally consist of an intense peak at low energy followed by a less intense peak at higher energies, the two peaks in the tissue spectra tend to be of a similar intensity (the ratio of the high-energy to low-energy peaks ranging from about 0.80 to 1.00).

In the absence of useful linear combination fits to the XANES spectra, principal component analysis offered an alternative method with which to analyse the spectra collected from the rat tissues. The speciation of Se in the tissues was not identified with this method, but comparisons between tissue types and different Se diets can be made. Figure 2e plots Se K-edge XANES spectra of tissues, cells and models, with the tissue spectra plotting mostly along the same axis as the cells and models. Ten outliers appear along an axis perpendicular to the model compound spectra. The Se concentration of the tissues from which these spectra were collected was very low leading to noisy spectra that interfered with their background subtraction and normalisation. Thus these spectra (Figure S1, supporting information), mainly from the thyroid, heart and red blood cells, were not included in further analyses.

Principal component analysis of model compound spectra

The exclusion of the extremely noisy spectra from consideration generated the scores plot presented in Figure 3. Two components explained 85% of the variance within the collection of the spectra. Principal Component 1 (PC1), which explained 75% of the variance, separated the highly reduced Se-bound model Se compounds from the highly oxidised O-bound model Se compounds. The loadings plot (Figure 3, inset) shows that these compounds are separated on the basis of the

energy of the first peak: the elemental Se peak at 12659 eV occurs at the opposite end of PC1 from the selenite peak at 12663 eV. PC2, which explains 11% of the variance, reflects, to some extent, the variation in the intensity of the peaks in the spectra, *c.f.* the sharp peaks of the C-bound Se model compounds *versus* the broad absorption maxima of the deprotonated Se model compounds (HSe^-, RSe^- and GPx).

The markedly different speciation of selenite-treated and selenoamino acid treated cells (described elsewhere[23-25]) is reflected in the separation of their spectra. The selenite-treated cells are associated with the inorganic Se–Se–Se, Se–Se and S–Se–S compounds, whereas the selenoamino acid treated cells are associated with the R–Se–R and R–Se–H species. The tissues of selenite-fed rats lie between and slightly overlap the two cancer cell populations. Also within this region, is the spectrum of a pellet of 1 μM selenite-treated human lung cancer cells that, like the rat tissue spectra, was poorly fit by a linear combination of model compound spectra.[24] The position of the rat tissue spectra in relation to model compounds suggests a mixture of species including diselenides, selenotrisulfides and deprotonated selenoamino acids (likely protein-bound), which is in accord with the fits of Se–Se and Se–S to the EXAFS of liver and kidney tissues (Table 1).

Careful inspection of the cancer cell spectra (Figure 4) revealed that the third principal component (PC3), which explains only 4% of the variance between the spectra is highly significant in this instance, given the separation of SeMet- and MeSeCys-treated cells by this component. This separation is not apparent in the second principal component (data not shown). PC3 describes the variation in the peak position and intensity of the second peak in the XAS spectrum. The MeSeCys-treated cells plot closer to the diselenide spectrum than the SeMet-treated cells, reflecting the presence of a small, but significant component of diselenide in the MeSeCys-treated cells as confirmed by fitting of XANES and EXAFS spectra.[23,25]

EXAFS and XANES analysis of tissues from selenite-treated rats

Due to the ability to fit EXAFS spectra *a priori* some speciation information is available from those spectra. The Se concentrations were highest in kidney and liver tissues of rats fed the 5 ppm Se diet (based on the relative signal strength of the raw XAS data; note also the lower noise levels in these spectra) and only these tissues had sufficient Se concentrations for the collection and analysis of EXAFS spectra. The parameters fit to the spectra are reported in Table 1 and selected fits are shown in Figure 5. Se scatterers were fitted to both the kidney and liver spectra. The tissues differed in that a Se scatterer alone provided a good fit to the liver spectrum, but the addition of a S scatterer improved the fit to the kidney spectrum. A multiple scattering Se–Se–Se fit to the liver

EXAFS was attempted, but did not improve on the single scattering fit (*i.e.* it did not account for the small peak observed at 3.25 Å in the Fourier Transform of Figure 5b). In a recent publication, we investigated the possibility of the formation of a Cu–Se species in kidney tissues, but analysis of Cu *K*-edge EXAFS in addition to Se *K*-edge EXAFS indicated that the presence of a Cu–Se species was unlikely.[34]

Previous attempts to determine Se speciation in the kidney and liver of rats fed Se supplemented diets have focused on the identification of selenoproteins (Se–C species), excretory compounds (Se–C species) and the fraction of unmetabolised treatment compound.[19-21] The EXAFS spectra of the liver and kidney of rats fed the high Se diet indicate the presence of Se–Se–Se and/or diselenide species in both spectra, as well as the presence of Se–S species in the kidney. We recognise that the total value of $N = 3$ (two Se–Se bonds and one Se–S bond) is chemically unlikely (the trimethylselenonium ion ($SeMe_3^+$) has a coordination number of three, but neither XANES nor PCA identifies it as a likely component). Attempts at constraining the total coordination number to the more likely $N = 2$ produced physically unrealistic fits or fits that failed to converge. It should be recognised that the determination of coordination numbers by single scattering analysis of EXAFS lacks accuracy (with errors in the order of 20%)[26] and, as such, the relative contribution of each scatterer to the total coordination number is most relevant in these fits to the EXAFS spectra.

The XANES spectra of the 5 ppm kidneys support the EXAFS data due to the position of the first peak at 12660.3 eV, much closer to the elemental Se (Se–Se–Se) peak at 12659.7 eV than the control kidney spectrum at 12661.4 eV (Figure 2a), although we do not have definitive evidence for the presence of elemental Se. The different mean Se–Se bond lengths calculated for the kidney (2.37 Å) and liver (2.34 Å) (Table 1), and the difference in amplitudes of their EXAFS spectra, suggest a different mixture of Se–Se species in each of those tissues. The Se scatterers, due to their relatively high mass, dominate the EXAFS spectra, most likely masking the presence of relatively low mass C scatterers. The XANES spectra, however, do indicate the presence of C-bound Se species: PCA showed that the XANES spectra of Se in rat tissues lay partway between the spectra of the Se–Se/Se–S and Se–C models in scores plots, implying that Se speciation in rats is a mixture of inorganic Se–Se and Se–S species and organic Se–C species (Figure 3).

We have previously reported the presence of diselenide, elemental Se and S-bound Se species in human lung cancer cells treated with 5 μM selenite for 24 h, as determined by analysis of XANES and EXAFS spectra of the freeze-dried samples.[24] Cancer cell lines are commonly used as models of selenium metabolism due to the interest anti-cancer activities of selenium compounds. Direct comparison of the XANES spectra collected from the frozen, hydrated rat tissues with those

collected from selenite-treated A549 lung cancer cells underscored the differences between these two models of Se metabolism. The lower-intensity peaks of the spectra collected from the rat tissues suggest that the tissues contain a lower proportion of inorganic Se compounds than the selenite-treated cells. The scores plots of these spectra reflected this with the plotting of the selenite-treated cell spectra amongst the spectra of the inorganic species. The difference in selenium speciation between the selenite-treated cancer cells and tissues from selenite-treated rats, may be explained by the substantial biological differences between the two models – particularly in the tissues from which the cancer cells were originally derived and the greater complexity of the animal model. Despite these differences between cancer cell and animal models, the presence of Se–Se and Se–S species in the rat kidney indicates that the reductive metabolism pathway, by which Se is reduced via GSSeSG, is active in both models. Similarly the formation of elemental Se, possibly via the oxidation of selenide and other unstable intermediates along the reductive metabolism pathway,[28] may occur in the liver and kidney as well as in the lung cancer cells.

Selenotrisulfides (S–Se–S) have been identified in the cytosolic fractions of liver from rats given a single intraperitoneal dose of selenite at 3 mL kg^{-1} body weight.[35] A selenosugar, glutathionylseleno-N-acetylgalactosamine, has been identified in rat liver,[19] but not in the kidneys. To the best of our knowledge, there are no previous reports of diselenide species found *in vivo* after Se supplementation, nor of selenotrisulfide species in rat kidneys. Recently, Loeschner *et al.* reported the presence of elemental selenium in the liver (17% of total Se) and kidneys (40% of total Se) of rats fed 0.5 mg Se as selenite per kg of body weight per day for 28 days.[36] The species was detected by anion exchange HPLC and ICP-MS after being reduced *in situ* with sodium sulfite to the selenosulfate anion. Elemental Se was also detectable in the liver and kidneys of rats fed control and low Se diets, although at much lower concentrations (<10% of total Se). The authors hypothesised that a change in metabolism occurs between rats fed low and high Se diets, leading to greater accumulation of elemental Se, presumably due to the exhaustion of GSH available to maintain the reductive metabolism of selenite (however GSH levels were not measured).

Se speciation in other tissues

The similarity of the XANES spectra collected from the heart, spleen, testis and red blood cells indicates that these organs all share a similar Se speciation profile. The intra- and inter-tissue similarity in these organs is in contrast to the varied Se speciation in the liver and kidney. Selenium speciation has been examined primarily in the urine,[37] in blood and serum, the liver and kidneys.[19,20,22] Suzuki *et al.* have also investigated Se speciation in the pancreas and lung.[19] There is no information on Se speciation in the heart, spleen and testis. The important role of Se in male

reproductive health and the potential role of Se in preventing and ameliorating the effects of cardiovascular disease indicate that efforts must be made to determine Se speciation in these organs. Interestingly, the XANES spectra of the control and 5 ppm Se testes were different (Figure 2c – for comparison, there was no change in the spleen). A change in Se speciation with Se supplementation may reflect the importance of Se to this organ (the selenoproteins GPx4[38] and SelP[39] are crucial in sperm development), although selenised yeast supplementation did not affect testicular Se status or semen quality in men taking a selenised yeast supplement,[40] nor did supplementation of mice with 0.8 ppm Se for 8 weeks alter GPx4 mRNA levels in the testis.[41] Studies aimed at determining the speciation of Se in the testis and heart – with and without dietary Se supplementation – are required.

Further studies required into Se speciation in the heart and testis would prove challenging for XAS. The difficulty of using XAS for speciation in biological samples is two-fold: the low concentration of Se in the samples necessitates long data acquisition times in order to collect enough spectra to average and significantly increase the signal to noise ratio and, a number of replicate samples need to be collected for each tissue to account for biological variation. Our experience indicates that the species of Se present in these samples are not susceptible to rapid photoreduction and so long data acquisition times are feasible. Further collection and analysis of XANES spectra of heart and testis samples is possible, and may be more powerful when combined with HPLC-ICP-MS analysis.

Principal component analysis

Principal component analysis is often used in combination with target transformation to determine the number and type of model compound spectra required to fit in linear combination to a sample XANES spectrum.[42-44] This process is the preferred method of analysing XANES spectra and it allows the quantification of different chemical species in individual samples. However, the method was not effective with this dataset. Likely model compounds from our extensive selenium model compound library (Figure 2d) were identified by target transformation, but poor fits to many of the experimental spectra were given by linear combination analysis using the targeted models. Thus we were unable to use this method to compare the proportions of selenium species present in the tissues. The large number of samples and variables made it difficult to draw conclusions by visual comparison of XANES spectra, as might be possible with a smaller dataset.

Alternative means of analysing XAS data are possible: a combination of PCA and linear discriminant analysis has been applied to sulfur X-ray absorption spectra collected from embryonic corneas to measure changes in sulfur speciation with corneal development.[45] In our experiments,

principal component analysis with the generation of scores and loadings plots provided a means of visualizing and objectively comparing the several dozen XANES spectra collected from rat tissues and cells. In traditional XAS analysis, PCA is conducted with experimental spectra only – not with model compound spectra. However, the inclusion of model compound spectra in the PCA provided essential context to scores and loadings plots. Inclusion of the model compound spectra allowed us to make sense of the principal components using the scores and loading plots (i.e. PC1 described the variation in the position of the first peak and PC2 described the variation in the intensity of the first peak). The model compounds also defined the space in which the sample spectra resided. By comparing the location of the samples to those of the models in the scores plots, we gained an understanding of how selenium speciation differed between the rat tissues and the cell samples (Figure 3) and between cells treated with different selenium compounds (Figure 4).

Our library of model Se compounds (Figure 2d) contains a wide array of biologically relevant Se coordination environments and we are uncertain as to which specie(s) could be added to improve the XANES fits. The missing components(s) must lie in the same space as the 3 week tissue samples, which themselves lie somewhat outside of the space bound by the model compound spectra. Principal component analysis could not separate tissue spectra on the basis of tissue type or concentration of selenite in the diet (Figure 6), although the tissues other than liver and kidney were loosely grouped, reflecting their similar XANES spectra. The tissues could be separated on the basis of the duration of the diets (Figure 6c) – whether from control or high Se diets, PCA clearly separated tissues into diets of 3 weeks' duration and 6 weeks' duration. Beamline conditions can be a source of variation and it has been noted that collection of data from the same beamline under the same conditions with a similar noise level is ideal,[42] if not always feasible when collecting data sets over an extended period of time from low Se concentrations samples. However, we can reject beamline conditions as a significant source of variation in this experiment: although spectra were collected across two different sets of beamtime, samples from each group were collected across the different beam times.

The change in speciation between diets of 3 and 6 weeks' duration, combined with the change in concentration of Se we noted earlier, may be indicative of an adaptation of the rats to the diets (both control and high Se diets) over time. A plateau in serum Se levels and a gradual decrease in liver Se levels has previously been observed in rats supplemented with 1 ppm selenite (0.5 ppm Se) or 5 ppm selenite (2.3 ppm Se) for 10 weeks.[46] In those experiments, serum Se content increased within 1 day of treatment and remained at the same level for the remainder of the 10 weeks. The Se content of the liver had the same rapid response and no further increase was observed, in fact a

slight decrease occurred after 4 weeks. The authors suggested that this was indicative of the rats adapting to the Se-supplemented diet. In the case of the experiments discussed herein, the ability of the rats to clear Se from their system may have improved between the diets of 3 and 6 weeks' duration, but whatever Se remained had an adverse impact on the rats – at least in terms of body weight measured at 6 weeks, which was significantly lower in the rats in the 5 ppm Se group than in the control rats ($P < 0.05$, as determined by two-tailed Student's *t*-test assuming equal variance). Although lower after 3 weeks, there was no significant difference between the weights of the rats on the 5 ppm Se diet and the controls after a diet of this duration. In another experiment, rats fed 2 ppm selenite for between 2 and 4 weeks, body and kidney weight loss was observed, as were histological indicators of damage and necrosis in the renal cortex.[47]

The intended use of PCA here – to identify relationships between Se speciation and tissue type, Se dose and duration of diet – was met only for the latter. In the small number of samples, biological variation between individual rats is likely to be a greater source of variance than Se dose and tissue type.

Conclusion

We have examined Se speciation in rat tissues by analysis of EXAFS spectra and the comparison of tissues XANES spectra to those of Se-treated cells and Se model compounds. EXAFS analysis indicated the presence of Se–Se (diselenides and/or elemental Se) and Se–S species in both liver and kidney tissues. Information about the presence of Se–C species was retained in the XANES spectra of the rat tissues. Species identified by HPLC-ICP-MS studies in rats, to date, are almost exclusively organic Se–C species with some Se–S species and one report of elemental Se. EXAFS may be particularly useful in identifying the inorganic selenium species, due to its lack of sample preparation requirements that reduce the risk of speciation artefacts and allows the identification of Se species in any form in a single sample using a single method of sample preparation and analysis.

X-ray absorption spectroscopy indicates that both selenite-treated cells and the tissues from selenite-fed rats are composed of Se-bound, S-bound and C-bound selenium species, yet the obvious differences in the XANES spectra of the cells and tissues strongly suggest that the proportions and exact identities of the selenium species in these samples differs. Given the selenium metabolites are responsible for the observed biological activities of selenium supplements,[48] this difference between the speciation of selenium in cancer cells *versus* the speciation in tissues underscores the importance of knowing the speciation of selenium in a model system to fully

understand how the selenium supplement is acting in that system.

Although it appears that most variation in the rat tissue samples is due to variation between individual rats, there is evidence that Se speciation changes between 3 week and 6 week diets – including the control (~0.3 ppm Se) diets. Selenium status is known to change with age, in particular, a decline in selenium status has been documented in the elderly,[49,50] and rats appear to adapt in response to long-term selenium supplementation.[46,51] The interest in long-term selenium supplementation as a chemoprevention measure,[52] or short to medium-term treatment with selenium as an adjuvant therapy,[53,54] requires more investigations of the changes of selenium status and speciation with age and duration of selenium supplementation.

Principal Component Analysis has proved to be a useful tool for comparing XANES spectra where linear combination fitting of model compounds fails. The addition of more sample spectra to the collection would increase the power of PCA by reducing the relative contribution of biological variations in individual rats to sample variance. Once the speciation of Se in normal rat tissues is established, the investigation of Se speciation in disease models can be made. The Se species present in rats fed selenoamino acid diets would also be of interest given the popularity of organic Se compounds in Se supplements (usually SeMet) and the chemopreventative properties of MeSeCys and MeSeA. Finally, a more direct comparison between a cell culture model and animal model requires experiments in primary hepatocytes and nephrocytes, or in hepatic or renal cancer models.

Acknowledgements

Graham N. George (University of Saskatchewan) provided Se K-edge X-ray absorption spectra of model Se compounds (except MeSeCys and GPx). Portions of this research were carried out at the Stanford Synchrotron Radiation Lightsource, a Directorate of SLAC National Accelerator Laboratory and an Office of Science User Facility operated for the U.S. Department of Energy Office of Science by Stanford University. The SSRL Structural Molecular Biology Program is supported by the DOE Office of Biological and Environmental Research, and by the National Institutes of Health, National Center for Research Resources, Biomedical Technology Program (P41RR001209). We acknowledge travel funding provided by the International Synchrotron Access Program (ISAP) managed by the Australian Synchrotron and funded by the Australian Government, research funding from the Australian Research Council (DP0985807 to HHH) and the Australian Synchrotron Postgraduate Award (CMW).

References

1. L. V. Papp, J. Lu, A. Holmgren, and K. K. Khanna, *Antioxid. Redox Signal.*, 2007, **9**, 775–806.
2. R. Irons, B. A. Carlson, D. L. Hatfield, and C. D. Davis, *J. Nutr.*, 2006, **136**, 1311–1317.
3. T. Yamaguchi, K. Sano, K. Takakura, I. Saito, Y. Shinohara, T. Asano, and H. Yasuhara, *Stroke*, 1998, **29**, 12–17.
4. L. C. Clark, G. F. Combs, B. W. Turnbull, E. H. Slate, D. K. Chalker, J. Chow, L. S. Davis, R. A. Glover, G. F. Graham, E. G. Gross, A. Krongrad, J. L. Lesher, H. K. Park, B. B. Sanders, C. L. Smith, and J. R. Taylor, *JAMA*, 1996, **276**, 1957–1963.
5. L. Wang, M. J. L. Bonorden, G. X. Li, H. J. Lee, H. Hu, Y. Zhang, J. D. Liao, M. P. Cleary, and J. Lu, *Cancer Prev. Res.*, 2009, **2**, 484–495.
6. N. Alwahaibi, J. Mohamed, and A. Alhamadani, *J. Trace Elem. Med. Biol.*, 2010, **24**, 119–123.
7. G. Flores-Mateo, A. Navas-Acien, R. Pastor-Barriuso, and E. Guallar, *Am. J. Clin. Nutr.*, 2006, **84**, 762–773.
8. G. Dennert, M. Zwahlen, M. Brinkman, M. Vinceti, M. P. A. Zeegers, and M. Horneber, *Cochrane Database Syst. Rev.*, 2012, CD005195.
9. R. Hurst, L. Hooper, T. Norat, R. Lau, D. Aune, D. C. Greenwood, R. Vieira, R. Collings, L. J. Harvey, J. A. Sterne, R. Beynon, J. Savovic, and S. J. Fairweather-Tait, *Am. J. Clin. Nutr.*, 2012, **96**, 111–122.
10. C. Ip, *J. Nutr.*, 1998, **128**, 1845–1854.
11. C. M. Weekley, J. Aitken, L. A. Finney, S. Vogt, P. Witting, and H. Harris, *Nutrients*, 2013, **5**, 1734–1756.
12. D. L. Hatfield, M.-H. Yoo, B. A. Carlson, and V. N. Gladyshev, *Biochim. Biophys. Acta*, 2009, **1790**, 1541–1545.
13. L. Björkhem-Bergman, U.-B. Torndal, S. Eken, C. Nyström, A. Capitano, E. H. Larsen, M. Björnstedt, and L. C. Eriksson, *Carcinogenesis*, 2005, **26**, 125–131.
14. L. Yan and L. C. DeMars, *Int. J. Cancer*, 2011, **131**, 1260–1266.
15. B. Gammelgaard, C. Gabel-Jensen, S. Stürup, and H. R. Hansen, *Anal. Bioanal. Chem.*, 2008, **390**, 1691–1706.
16. B. Gammelgaard, M. I. Jackson, and C. Gabel-Jensen, *Anal. Bioanal. Chem.*, 2011, **399**, 1743–1763.
17. C. Gabel-Jensen and B. Gammelgaard, *J. Anal. At. Spectrom.*, 2010, **25**, 414–418.
18. K. Lunøe, C. Gabel-Jensen, S. Stürup, L. Andresen, S. Skov, and B. Gammelgaard, *Metallomics*, 2011, **3**, 162–168.
19. K. T. Suzuki, Y. Ohta, and N. Suzuki, *Toxicol. Appl. Pharmacol.*, 2006, **217**, 51–62.
20. K. T. Suzuki, C. Doi, and N. Suzuki, *Toxicol. Appl. Pharmacol.*, 2006, **217**, 185–195.
21. Y. Suzuki, Y. Hashiura, T. Sakai, T. Yamamoto, T. Matsukawa, A. Shinohara, and N. Furuta, *Metallomics*, 2013, **5**, 445.
22. Y. Tsuji, N. Suzuki, K. T. Suzuki, and Y. Ogra, *J. Toxicol. Sci.*, 2009, **34**, 191–200.
23. C. M. Weekley, J. B. Aitken, S. Vogt, L. A. Finney, D. J. Paterson, M. D. de Jonge, D. L. Howard, I. F. Musgrave, and H. H. Harris, *Biochemistry*, 2011, **50**, 1641–1650.
24. C. M. Weekley, J. B. Aitken, S. Vogt, L. A. Finney, D. J. Paterson, M. D. de Jonge, D. L. Howard, P. K. Witting, I. F. Musgrave, and H. H. Harris, *J. Am. Chem. Soc.*, 2011, **133**, 18272–18279.
25. C. M. Weekley, J. B. Aitken, I. F. Musgrave, and H. H. Harris, *Biochemistry*, 2012, **51**, 736–738.
26. G. N. George, B. Hedman, and K. O. Hodgson, *Nat. Struct. Biol.*, 1998, **5**, 645–647.
27. H. S. Hsieh and H. E. Ganther, *Biochemistry*, 1975, **14**, 1632–1636.
28. H. E. Ganther, *Biochemistry*, 1971, **10**, 4089–4098.

29. S. Kumar, M. Björnstedt, and A. Holmgren, *Eur. J. Biochem.*, 1992, **207**, 435–439.
30. M. Björnstedt, S. Kumar, and A. Holmgren, *J. Biol. Chem.*, 1992, **267**, 8030–8034.
31. M. Wallenberg, E. Olm, C. Hebert, M. Björnstedt, and A. P. Fernandes, *Biochem. J.*, 2010, **429**, 85–93.
32. J. T. Deagen, J. A. Butler, M. A. Beilstein, and P. D. Whanger, *J. Nutr.*, 1987, **117**, 91–98.
33. Y. Shiobara, Y. Ogra, and K. T. Suzuki, *Life Sci.*, 2000, **67**, 3041–3049.
34. C. M. Weekley, A. Shanu, J. B. Aitken, S. Vogt, P. K. Witting, and H. Harris, *Metallomics*, 2014.
35. P. Braga, M. Montes-Bayón, J. Alvarez, J. M. López, and A. Sanz-Medel, *J. Anal. At. Spectrom.*, 2004, **19**, 1128–1133.
36. K. Loeschner, N. Hadrup, M. Hansen, S. A. Pereira, B. Gammelgaard, L. H. Møller, A. Mortensen, H. R. Lam, and E. H. Larsen, *Metallomics*, 2014, **6**, 330.
37. T. Jäger, H. Drexler, and T. Göen, *J. Anal. At. Spectrom.*, 2013, **28**, 1402.
38. L. Flohé, *Biol. Chem.*, 2007, **388**, 987–995.
39. G. E. Olson, V. P. Winfrey, S. K. Nagdas, K. E. Hill, and R. F. Burk, *Biol. Reprod.*, 2005, **73**, 201–211.
40. W. C. Hawkes, Z. Alkan, and K. Wong, *J. Androl.*, 2009, **30**, 525–533.
41. Q. Zhang, L. Chen, K. Guo, L. Zheng, B. Liu, W. Yu, C. Guo, Z. Liu, Y. Chen, and Z. Tang, *Biol. Trace Elem. Res.*, 2013.
42. S. Beauchemin, D. Hesterberg, and M. Beauchemin, *Soil Science Society of America Journal*, 2002, **66**, 83–91.
43. A. Gaur and B. D. Shrivastava, *Spectrosc. Lett.*, 2013, **46**, 375–383.
44. J. Essilfie-Dughan, I. J. Pickering, M. J. Hendry, G. N. George, and T. Kotzer, *Environ. Sci. Technol.*, 2011, **45**, 455–460.
45. E. Koudouna, G. Veronesi, I. I. Patel, M. Cotte, C. Knupp, F. L. Martin, and A. J. Quantock, *Biophys. J.*, 2012, **103**, 357–364.
46. S. Erkhembayar, A. Mollbrink, M. Eriksson, E. H. Larsen, and L. C. Eriksson, *J. Trace Elem. Med. Biol.*, 2011, **25**, 254–259.
47. A. M. Hussein, H. A. Saleh, and M. H. N, *Tissue and Cell*, 2014, **46**, 170–177.
48. C. M. Weekley and H. H. Harris, *Chem. Soc. Rev.*, 2013, **42**, 8870–8894.
49. O. Olivieri, A. M. Stanzial, D. Girelli, M. T. Trevisan, P. Guarini, M. Terzi, S. Caffi, F. Fontana, M. Casaril, and S. Ferrari, *Am. J. Clin. Nutr.*, 1994, **60**, 510–517.
50. J. Arnaud, N. T. Akbaraly, I. Hininger, A.-M. Roussel, and C. Berr, *J. Nutr. Biochem.*, 2007, **18**, 482–487.
51. M. Janghorbani, S. Rockway, C. S. Mooers, E. M. Roberts, B. T. Ting, and M. D. Sitrin, *J. Nutr.*, 1990, **120**, 274.
52. L. C. Clark, B. Dalkin, A. Krongrad, G. F. Combs, B. W. Turnbull, E. H. Slate, R. Witherington, J. H. Herlong, E. Janosko, D. Carpenter, C. Borosso, S. Falk, and J. Rounder, *Br. J. Urol.*, 1998, **81**, 730–734.
53. N.-P. Becker, J. Martitz, K. Renko, M. Stoedter, S. Hybsier, T. Cramer, and L. Schomburg, *Metallomics*, 2014.
54. H. A. Meyer, T. Endermann, C. Stephan, M. Stoedter, T. Behrends, I. Wolff, K. Jung, and L. Schomburg, *PLoS ONE*, 2012, **7**, e46644.

Tables

Table 1. Parameter of single scattering fits to Se K-edge EXAFS spectra of liver and kidney from rats fed a 5 ppm Se (as selenite) diet for 3 weeks.

tissue	bond	coordination number (N)	interatomic distance (R)	Debye-Waller factor (σ^2, Å^{-2})	$-\Delta E_0$ (eV)	fit error
kidney	Se	2	2.373(5)	0.0038(1)	6(2)	30%
	S	1	2.21(2)	0.006(1)		
liver	Se	2	2.342(6)	0.0060(2)	15(2)	59%

[a]The k-range was 1 – 14.2 Å^{-1} and a scale factor (S_0^2) of 0.9 was used for all fits. $\Delta E_0 = E_0 - 12658$ eV where E_0 is the threshold energy. Values in parentheses are the estimated standard deviation derived from the diagonal elements of the covariance matrix and are a measure of precision. The fit-error is defined as $[\Sigma k^6(\chi_{exp}-\chi_{calc})^2/\Sigma k^6\chi_{exp}^2]^{½}$.